NeuroImage: Clinical 28 (2020) 102408

Contents lists available at ScienceDirect

NeuroImage: Clinical

journal homepage: www.elsevier.com/locate/ynicl

Gait initiation in progressive supranuclear palsy: brain metabolic correlates

Chiara Palmisano[a,b], Massimiliano Todisco[a,c,d], Giorgio Marotta[e], Jens Volkmann[a], Claudio Pacchetti[c], Carlo A. Frigo[b], Gianni Pezzoli[f], Ioannis U. Isaias[a,*]

[a] Department of Neurology, University Hospital of Würzburg and Julius Maximilian University of Würzburg, Würzburg, Germany
[b] MBMC Lab, Department of Electronics, Information and Bioengineering, Politecnico di Milano, Milan, Italy
[c] Parkinson's Disease and Movement Disorders Unit, IRCCS Mondino Foundation, Pavia, Italy
[d] Department of Brain and Behavioral Sciences, University of Pavia, Pavia, Italy
[e] Department of Nuclear Medicine, Fondazione IRCCS Ca' Granda – Ospedale Maggiore Policlinico, Milan, Italy
[f] Centro Parkinson ASST G. Pini-CTO, Milan, Italy

ARTICLE INFO

Keywords:
Anticipatory postural adjustments
Gait initiation
Positron emission tomography
Progressive supranuclear palsy

ABSTRACT

The initiation of gait is a highly challenging task for the balance control system, and can be used to investigate the neural control of upright posture maintenance during whole-body movement. Gait initiation is a centrally-mediated motion achieved in a principled, controlled manner, including predictive mechanisms (anticipatory postural adjustments, APA) that destabilize the antigravitary postural set of body segments for the execution of functionally-optimized stepping. Progressive supranuclear palsy (PSP) is a neurodegenerative disease characterized by early impairment of balance and frequent falls. The neural correlates of postural imbalance and falls in PSP are largely unknown. We biomechanically assessed the APA at gait initiation (imbalance, unloading, and stepping phases) of 26 patients with PSP and 14 age-matched healthy controls. Fourteen of 26 enrolled patients were able to perform valid gait initiation trials. The influence of anthropometric and base-of-support measurements on the biomechanical outcome variables was assessed and removed. Biomechanical data were correlated with clinical findings and, in 11 patients, with brain metabolic abnormalities measured using positron emission tomography and 2-deoxy-2-[18F]fluoro-D-glucose. Patients with PSP showed impaired modulation of the center of pressure displacement for a proper setting of the center of mass momentum and subsequent efficient stepping. Biomechanical measurements correlated with "Limb motor" and "Gait and midline" subscores of the Progressive Supranuclear Palsy Rating Scale. Decreased regional glucose uptake in the caudate nucleus correlated with impaired APA programming. Hypometabolism of the caudate nucleus, supplementary motor area, cingulate cortex, thalamus, and midbrain was associated with specific biomechanical resultants of APA. Our findings show that postural instability at gait initiation in patients with PSP correlates with deficient APA production, and is associated with multiple and distinctive dysfunctioning of different areas of the supraspinal locomotor network. Objective biomechanical measures can help to understand fall-related pathophysiological mechanisms and to better monitor disease progression and new interventions.

1. Introduction

The earliest and most disabling symptom of progressive supranuclear palsy (PSP) relates to gait and balance impairment. The uncompensated loss of postural reflexes, coupled with a peculiar lack of awareness of the difficulties with equilibrium, leads to frequent fall and injuries. This marked postural instability has been related to a combination of visual-vestibular impairment, axial rigidity, bradykinesia, and impaired postural reflexes, but the anatomical correlates are still largely unknown. The paucity of information regarding postural control in PSP patients greatly limits our understanding of the underlying pathophysiological mechanisms and the possibility of monitoring disease progression and the effects of disease-specific therapeutic options (Canesi et al., 2016; Clerici et al., 2017; Giordano et al., 2014).

The initiation of gait is known to be a highly challenging task for the balance control system, and is classically used in the literature to investigate how the central nervous system controls balance during a whole-body movement (Isaias et al., 2014; Yiou et al., 2017). Gait initiation (GI) is a centrally-mediated motion achieved in a principled, controlled manner including feedforward signals for generating anticipatory postural adjustments (APA), i.e., muscular synergies that precede and accompany the transition between quiet stance and steady-

* Corresponding author: University Hospital of Würzburg, Josef-Schneider-Str. 11, 97080 Würzburg, Germany.
E-mail address: Isaias_I@ukw.de (I.U. Isaias).

https://doi.org/10.1016/j.nicl.2020.102408
Received 20 April 2020; Received in revised form 29 July 2020; Accepted 30 August 2020
Available online 02 September 2020

state locomotion (Jacobs et al., 2009; Palmisano et al., 2020; Richard et al., 2017; Farinelli et al., 2020). The production of APA at GI specifically aims to destabilize the antigravitary postural set via misalignment between the center of pressure (CoP) and the center of mass (CoM) (Crenna et al., 2006). This CoP-CoM offset during the imbalance phase (IMB) produces a gravitational moment favoring CoM forward acceleration. The displacement of the CoP under the stance foot during the unloading phase (UNL) allows the swing foot to clear the ground for the execution of a functionally-optimized step. APA have a significant role in the optimal motor performance of GI in terms of forward propulsion and stability (McIlroy and Maki, 1999), and may represent a direct measurement of the integrity of feedforward processing of the supraspinal locomotor network (Jacobs et al., 2009; Yiou et al., 2017).

Only two studies have previously investigated the GI task in patients with PSP. In these patients, Welter and coll. showed poor braking capacity during the stepping phase, with the CoM mechanically arrested by the swing limb at heel contact (Welter et al., 2007). Amano and coll. described a diminished anteroposterior (AP) shift of the CoP in PSP patients during the IMB, which resulted in a reduced CoP-CoM moment arm. Of note, in both studies patients were evaluated only on dopaminergic medication, which can significantly affect motor behavior at GI (Palmisano et al., 2020). Furthermore, the influence of anthropometric measurements (AM) and base of support (BoS) on the GI performance was not taken into account in these studies (Palmisano et al., 2020; Rocchi et al., 2006). A third study (Zwergal et al., 2011) correlated posturographic findings of PSP patients with brain metabolic abnormalities measured with positron emission tomography (PET) and 2-deoxy-2-[18F]fluoro-D-glucose ([18F]FDG). The authors showed a significant role of the thalamus and caudate nucleus in the maintenance of balance in PSP, especially in conditions with somatosensory modulation (Zwergal et al., 2011). In general, PET with [18F]FDG has consistently revealed reduced glucose metabolism in the frontal and cingulate cortex, thalamus, caudate nucleus, and midbrain of PSP patients (Eckert et al., 2005; Foster et al., 1988; Karbe et al., 1992; Zwergal et al., 2011).

In our study, we aimed to deepen our understanding of the pathophysiology of balance impairment in patients with PSP. We first defined biomechanical alterations of GI in these patients, considering the influence of AM and BoS. We then explored the correlations of several biomechanical parameters with clinical features and PET with [18F]FDG findings.

2. Materials and methods

2.1. Participants

We recruited 26 patients with probable PSP and 14 age-matched healthy controls (HC). PSP was diagnosed according to the Movement Disorder Society criteria (Höglinger et al., 2017). All patients were clinically classified as Richardson's syndrome (PSP-RS) as they predominantly showed early-onset postural instability in addition to oculomotor dysfunction (Respondek et al., 2014). Exclusion criteria were neurological diseases other than PSP, vestibular disorders, cardiovascular diseases, diabetes mellitus, orthopedic problems, or past major orthopedic surgery. None of the recruited patients suffered from freezing of gait. A neurologist expert in movement disorders (IUI) clinically evaluated all patients using the Progressive Supranuclear Palsy Rating Scale (PSPRS), comprising six areas: History, Mentation, Bulbar, Ocular motor, Limb motor, Gait and midline (Golbe and Ohman-Strickland, 2007). Eighteen patients were taking dopaminergic medications (levodopa equivalent daily dose range: 200–800 mg) with mild clinical benefits, mostly on akinetic-rigid symptoms. The clinical evaluation was performed in the morning, after overnight suspension of all dopaminergic drugs, and just before starting the biomechanical assessment. The local Ethics Committee approved the study and written informed consent was obtained from all patients.

2.2. Experimental setup

PSP patients were evaluated in the morning after overnight suspension of all dopaminergic drugs. All subjects performed at least three GI trials (range 3–7). For each subject, all variables were averaged over the trials. Ground reaction forces were measured using two dynamometric force plates (9286A, KISTLER, sampling frequency 960Hz). Kinematic data were recorded using a six-camera optoelectronic system (SMART 1.10, BTS, sampling frequency 60Hz), and kinematics was monitored using a full-body set of 29 retroreflective markers placed on anatomical landmarks, according to a published protocol (Isaias et al., 2012). Subjects were instructed to stand quietly on the force plates (one foot on each) with their eyes open and arms down by the side of the body for 30 s. Following a verbal cue, subjects waited for a self-selected time interval, then started walking with their preferred stepping leg at their own (spontaneous) pace. The feet position during initial standing was self-selected by each subject. Subjects were allowed to rest between trials. During the recordings, an examiner was always close to the patient, ready to intervene in case of loss of balance and thus prevent a fall. The examiner was positioned behind the subject (outside the visual field and with no physical contact) to avoid any interference with the execution of the GI task. We did not experience any fall-related adverse events during this study.

2.3. Anthropometric measurements and base of support assessment

The AM of each subject (body height [BH], inter anterior–superior iliac spines distance [IAD], limb length [LL], foot length [FL], body mass [BM], and body mass index [BMI]) were computed by means of an acquisition of 5 s of upright stance on the force plates with eight additional markers placed on the first metatarsi, medial malleoli, medial condyles, and trochanters (Palmisano et al., 2020). The BoS parameters were defined for each GI trial by the markers placed on the feet (Palmisano et al., 2020). We computed the BoS area as the area inside the markers on the feet, and the BoS width as the distance between the ankle centers, estimated as the middle points between the external and internal malleoli. Additionally, to evaluate the feet placement across trials and patients, we computed the anterior-posterior (AP) distance between the markers on the heels (foot alignment), the angles between the axis passing through the malleoli and the horizontal axis of the reference system of the laboratory for the left (βL) and right (βR) foot, and their difference (β_{DELTA}). We also calculated the BoS opening angle as the sum of βL and βR. The AM and BoS parameters and their abbreviations are listed in Table 1.

2.4. Gait initiation parameters

The CoP pathway was computed as the weighted mean of the signals recorded by the two force plates under the left and right foot:

$$CoP = \frac{CoP_L \times RV_L + CoP_R + RV_R}{RV_L + RV_R}$$

where CoP_L and CoP_R are the CoP of the left and right foot, respectively, and RV_L and RV_R are the vertical components of the ground reaction forces under the left and right foot, respectively (Winter, 1995). The resultant CoP track was filtered using a fifth-order, low-pass Butterworth filter (cut-off frequency: 30 Hz) (Palmisano et al., 2020). GI parameters were automatically extracted by means of ad hoc Matlab algorithms. We identified two main phases of APA (Fig. 1): the IMB (i.e., the first displacement of the CoP backwards and towards the swing limb), and the UNL (i.e., the subsequent CoP movement towards the stance limb) (Crenna et al., 2006; Palmisano et al., 2020). We evaluated the IMB and UNL duration and the key features of the CoP movement during these phases, such as CoP displacement and the average and maximum CoP velocity in the AP and mediolateral (ML) directions (complete list and description of parameters and abbreviations in

Table 1
Biomechanical parameters.

Acronym	Description	Decomposition
Anthropometric measurements		
BH	Body height (cm)	
IAD	Inter anterior–superior iliac spines distance (cm)	
FL	Foot length (cm)	
LL	Limb length (cm)	
BM	Body mass (kg)	
BMI	Body mass index (kg/m^2)	
Base of support		
BA	BoS area (cm^2)	
BoSW	BoS width (cm)	
FA	Foot alignment (cm)	
β_{DELTA}	Difference among feet extra-rotation angles (°)	
β	BoS opening angle, i.e., the sum of feet extra-rotation angles (°)	
Imbalance phase		
IMBT	Imbalance duration (s)	
IMBD	Imbalance CoP displacement (mm)	AP, ML
IMBAV	Imbalance CoP average velocity (mm/s)	AP, ML
IMBMV	Imbalance CoP maximal velocity (mm/s)	AP, ML
IMBCoMV	CoM velocity at imbalance end (mm/s)	
IMBCoMA	CoM acceleration at imbalance end (mm/s^2)	
IMBCoPCoM	CoP-CoM distance at imbalance end (mm)	
IMBSLOPE	Slope of CoP-CoM vector at imbalance end (°)	
Unloading phase		
UNLT	Unloading duration (s)	
UNLD	Unloading CoP displacement (mm)	AP, ML
UNLAV	Unloading CoP average velocity (mm/s)	AP, ML
UNLMV	Unloading CoP maximal velocity (mm/s)	AP, ML
UNLCoMV	CoM velocity at unloading end (mm/s)	
UNLCoMA	CoM acceleration at unloading end (mm/s^2)	
UNLCoPCoM	CoP-CoM distance at unloading end (mm)	
UNLSLOPE	Slope of CoP-CoM vector at unloading end (°)	
Stepping phase		
TOCoMV	CoM velocity at stance foot toe-off (mm/s)	
TOCoMA	CoM acceleration at stance foot toe-off (mm/s^2)	
TOCoPCoM	CoP-CoM distance at stance foot toe-off (mm)	
SL	First step length (mm)	
SAV	First step average velocity (mm/s)	
SMV	First step maximum velocity (mm/s)	

Of note, some measurements were additionally analyzed separately in the AP and ML directions, as indicated by the column "Decomposition". Abbreviations: AP = anterior-posterior, CoP = center of pressure, CoM = center of mass, ML = mediolateral.

Table 1). Kinematic data served for the evaluation of the first step (stepping phase) and the CoM movement. The coordinates of the markers were filtered using a fifth-order, low-pass Butterworth filter (cut-off frequency: 10 Hz) (Palmisano et al., 2019). For each trial, we evaluated the first step length, average and maximum velocity, computed based on the tracks of the markers placed on the heels. The whole-body CoM was calculated as described by Dipaola and coll. (Dipaola et al., 2016), based on the anthropometric tables and regression equations proposed by Zatsiorsky (Zatsiorsky, 2002). The position of the CoM with respect to the CoP and the CoM velocity and acceleration were evaluated at the end of the IMB and UNL and at stance foot toe-off. The slope of the vector connecting the CoP and the CoM was also computed at the end of the IMB and UNL, as a measurement of the direction of CoM acceleration at these critical points of APA execution. All GI parameters are described in Table 1.

2.5. PET data acquisitions and analysis

Of the 14 patients who performed valid GI trials, 11 underwent PET with [18F]FDG within three months of the biomechanical analysis. PET scans were performed using the PET/CT scanner Biograph Truepoint 64 (Siemens Healthineers) at the Fondazione IRCCS Ca' Granda – Ospedale Maggiore Policlinico, Milan. Patients fasted overnight and stayed in resting conditions in a dimly-lit and quiet room for 30 min between the injection of 150 ± 30 MBq [18F]FDG and a 15-min PET scan. CT scans for attenuation correction were acquired using a low-dose protocol. PET sections were reconstructed in the form of transaxial images of 256 × 256 pixels of 2 mm, employing an iterative algorithm (i.e., ordered subset expectation maximization [six iterations, eight subsets]). The resolution of the PET system was 4–5 mm full width at half maximum.

PET data were analyzed using the Statistical Parametric Mapping (SPM 12, Wellcome Department of Cognitive Neurology, London), with false discovery rate (FDR) correction for multiple testing ($p < 0.01$) and age at PET scan as nuisance covariate. Scans were spatially normalized to a [18F]FDG PET template in the standardized Montreal Neurological Institute (MNI) space (16 iterations, non-linear transformation and trilinear interpolation) and then smoothed with a 10-mm isotropic Gaussian filter to account for subtle variations in anatomic structures and to increase the signal-to-noise ratio. A second group of 12 age- and gender-matched HC, different from the healthy subjects recruited for the biomechanical assessment and previously acquired using the same PET protocol, served as the control group for the molecular imaging comparison (Isaias et al., 2020). Paired *t*-test applied to voxel-wise comparisons was used to recognize significant differences between PSP patients and controls. We considered the clusters with $k \geq 200$ voxels and threshold of $p < 0.05$ FWE-corrected as significant. Whole-brain analyses were followed by a post hoc volume of interest (VOI) analysis, using a spherical VOI (5 mm radius) centred on the peak voxel of significant clusters in SPM analysis and calculating the standardized uptake value ratio (SUVR) (i.e., mean count per voxel VOI/mean count per voxel global brain) of [18F]FDG uptake. For each VOI, we extracted the [18F]FDG uptake values that were divided by the

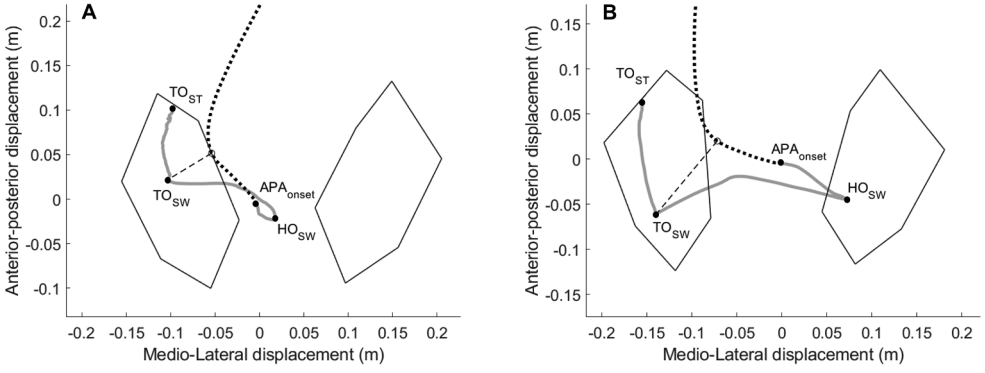

Fig. 1. Two-dimensional center of pressure and center of mass trajectories during gait initiation of one patient with PSP (A) and one HC (B). The center of pressure (CoP) and center of mass (CoM) excursions during gait initiation are depicted in the horizontal plane with a grey solid and a black dotted line, respectively. The black dashed line represents the CoP-CoM vector at the end of the unloading phase. As for the gait initiation (GI) task, two phases were analyzed separately: the anticipatory postural adjustments (APA) phase and the stepping phase. The APA phase was subdivided into two subphases called imbalance phase (IMB) and unloading phase (UNL). The imbalance phase goes from the instant APA_{onset}, at which the CoP starts moving backward and toward the swing foot, to the instant of heel-off of the swing foot (HO_{SW}). The unloading phase goes from HO_{SW} to the instant of toe-off of the swing foot (TO_{SW}). The stepping phase was evaluated by means of the marker placed on the heel of the leading foot and went from the heel-off to the instant of heel-strike (not in the figure). TO_{ST} is the instant of toe-off of the stance foot.

whole cortex uptake to reduce between-patient variability. The resulting [18F]FDG uptake ratios were then used to explore correlations with GI parameters.

2.6. Statistical analyses

Outlier values for each variable were identified using the Mahalanobis distance. To determine the influence of the AM and BoS on GI parameters, we performed a partial correlation analysis between the GI parameters and the AM controlling for the BoS, and between the GI parameters and the BoS controlling for the AM (Palmisano et al., 2020). GI parameters that correlated significantly with the BoS ($p < 0.01$ and Spearman's ρ correlation coefficient > 0.5) in one or both groups were excluded from further analyses. We opted for this cautious approach since the preferred BoS of each patient in the absence of the disease could not be known. GI parameters that significantly correlated with one or more AM in one or both groups were decorrelated as described by O'Malley (O'Malley, 1996). GI parameters independent from BoS and decorrelated from AM were compared between PSP patients and HC using Student's *t*-test or Wilcoxon rank-sum test as appropriate. The parameters that were significantly different between the two groups were correlated with clinical features and [18F]FDG uptake values with the Spearman's rank correlation coefficient. This analysis was limited to the PSP cohort, as we recruited different subjects for the biomechanical and imaging evaluations. We used the Bonferroni correction to adjust the statistical significance threshold for multiple comparisons. Statistical analyses were performed with JMP Pro (version 14.0, SAS Institute Inc.) or Matlab (Matlab® R2018b, The Mathworks Inc.).

3. Results

3.1. Study population

Of 26 patients with PSP, eight were excluded because of falls during the execution of the GI task (which occurred within the first 20 s of upright posture maintenance) and four because of the absence of the IMB. We did not find any differences between the remaining 14 PSP and HC patients regarding demographics or AM and BoS parameters (Table 2).

3.2. Influence of anthropometric measurements and base of support

In HC, the velocity, acceleration and position of the CoM with respect to the CoP at IMB end were influenced by AM and BoS parameters. In the same cohort, during the UNL the CoP displacement and the average and maximum velocity of the CoP in the ML direction were influenced by the BoS. In the PSP group, we did not find any correlations of GI parameters with BoS measurements. In Table 2, we list all the GI parameters not affected by the BoS in both groups.

3.3. Biomechanical differences between PSP patients and HC

Patients with PSP showed significant alterations in the GI task with respect to the HC group (Table 2). Of relevance, the kinematic resultants of APA in PSP patients were significantly reduced both in duration and amplitude, with a particular decrement in the AP measurements of the IMB. As a result, the CoM movement was significantly impaired in the PSP group as revealed by lower values of the velocity and acceleration of the CoM at the UNL end, as well as the velocity and position of the CoM with respect to the CoP at the stance foot toe-off. Patients with PSP also showed a significantly reduced first step length, average and maximum velocity compared to HC. Results were significant using the Bonferroni-corrected p-value threshold. Representative CoP and CoM excursions during GI are shown in Fig. 1.

3.4. Clinical findings and correlations in patients with PSP

The correlations of PSPRS subscores with GI parameters are listed in Table 3A. Of most relevance, we showed a significant correlation between the PSPRS subscores related to motor impairment (i.e., Limb motor, and Gait and midline) and the kinematic measurements of all GI phases, thus supporting both the validity of the PSPRS with respect to a precise biomechanical evaluation and the reliability of our findings in the context of a general clinical assessment. Results were significant only using the uncorrected p-value threshold ($p < 0.05$).

3.5. Glucose metabolism at rest in patients with PSP and biomechanical correlations

We identified six hypometabolic brain regions in the PSP group: the right dorsolateral prefrontal cortex (cluster peak coordinates: x = 46, y = 14, z = 50; k = 381, pFWEcorr = 0.005, Z-score = 4.43), the left supplementary motor area (SMA, cluster peak coordinates: x = -8, y = 18, z = 62, k = 221, pFWEcorr = 0.039, Z-score = 4.91), the middle cingulate cortex (cluster peak coordinates: x = 12, y = 4, z = 38, k = 493, pFWEcorr = 0.01, Z-score = 4.48), the left caudate nucleus (cluster peak coordinates: x = -14, y = 6, z = 12, k = 366, pFWEcorr = 0.006, Z-score = 6.76) the medial thalamus and the midbrain (cluster peak coordinates: x = 8, y = −20, z = 12, k = 2184, pFWEcorr < 0.001, Z-score = 6.31; subcluster peak coordinates: x = 8, y = -20, z = -12, pFWEcorr < 0.001, Z-score = 6.22, respectively) (Fig. 2).

Of relevance, in patients with PSP the [18F]FDG uptake of the caudate nucleus correlated positively with the CoP average velocity in the AP direction during the IMB (IMBAV AP), a key kinematic feature of APA pre-programming of the GI task (Table 3B, Fig. 3). The caudate nucleus, together with the middle cingulate cortex, correlated with the velocity of the CoM at the end of the UNL phase (UNLCoMV) and, together with the thalamus, with the distance between CoP and CoM at stance foot toe-off (TOCoPCoM) (Table 3B, Fig. 3). The TOCoPCoM also correlated with the midbrain [18F]FDG uptake. Finally, the SMA correlated with the slope of the CoP-CoM vector at the end of the UNL phase (UNLSLOPE) (Table 3B, Fig. 3). Results were significant only with the uncorrected p-value threshold ($p < 0.05$).

4. Discussion

Progressive supranuclear palsy is a neurodegenerative disorder with poor prognosis and no disease-modifying treatment. In these patients, objective biomechanical measures may help to clarify fall-related pathophysiological mechanisms to better explore disease progression and new interventions (Canesi et al., 2016; Clerici et al., 2017; Giordano et al., 2014). Also, a detailed biomechanical evaluation combined with brain imaging studies in patients with specific gait and balance disturbances may deepen our understanding of the supraspinal locomotor network.

The first result of our study is the absence in four patients of the IMB, which represents the main and first biomechanical resultant of APA directly governed by top-down feedforward motor control (Jacobs et al., 2009; Yiou et al., 2017). In agreement with Amano and coll. (Amano et al., 2015), this finding suggests a pronounced impairment of the ability to dynamically control balance as patients tend to move the CoP immediately toward the stance foot at the onset of GI (Fawver et al., 2018). The subsequent failure of quickly advancing the swing limb due to bradykinesia, together with a poor braking capacity (Welter et al., 2007), would dramatically increase the risk of fall in these patients.

In all the evaluated 14 patients, the kinematic resultants of the APA were reduced in amplitude and velocity, predominantly during the IMB. This yielded a reduced CoM velocity at the end of the UNL, and consequently at the stance foot toe-off, and a short and slow first step

Table 2
Demographic, clinical, and biomechanical data of patients with PSP and HC.

		PSP	HC	p-val
Demographic data	Gender (males/total)	6/14	9/14	0.256 [a]
	Age (years)	66.6 ± 4.7	65.1 ± 3.4	0.341[b]
Clinical features	Disease duration (years)	5.3 ± 3.1	–	–
	PSPRS History	5.5 ± 2.1	–	–
	PSPRS Mentation	1.4 ± 1.1	–	–
	PSPRS Bulbar	2.9 ± 1.3	–	–
	PSPRS Ocular motor	8.3 ± 4.8	–	–
	PSPRS Limb motor	5.6 ± 1.9	–	–
	PSPRS Gait and midline	9.3 ± 2.7	–	–
	PSPRS Total	33.0 ± 9.7	–	–
	LEDD (mg)	326.7 ± 304.0	–	–
Anthropometric measurements	BH (cm)	163.7 ± 8.9	169.4 ± 11.4	0.055[c]
	IAD (cm)	30.6 ± 5.2	28.6 ± 1.7	0.765[c]
	FL (cm)	24.3 ± 2.0	25.0 ± 1.5	0.316[b]
	LL (cm)	84.0 ± 6.6	88.9 ± 6.0	0.055[b]
	BM (kg)	72.3 ± 11.6	73.9 ± 13.2	0.738[b]
	BMI (kg/m^2)	27.2 ± 5.3	25.4 ± 3.7	0.314[b]
Base of support	BA (cm^2)	752.1 ± 113.4	721.8 ± 126.5	0.510[b]
	BoSW (cm)	197.8 ± 40.9	181.3 ± 51.1	0.353[b]
	FA (cm)	10.2 ± 6.0	7.1 ± 4.1	0.128[b]
	β_{DELTA} (°)	23.6 ± 6.8	21.4 ± 9.3	0.486[b]
	β (°)	21.3 ± 7.4	20.1 ± 8.4	0.675[b]
GI parameters	IMBT (s)	0.42 ± 0.20	0.38 ± 0.09	0.961[c]
	IMBD (mm)	22.3 ± 10.3	66.7 ± 23.9	< **0.001*** [c]
	IMBD AP (mm)	3.0 ± 7.7	41.1 ± 16.5	< **0.001*** [c]
	IMBD ML (mm)	18.2 ± 10.3	46.8 ± 18.5	< **0.001*** [c]
	IMBAV (mm/s)	64.0 ± 43.2	193.8 ± 87.1	< **0.001*** [b]
	IMBAV AP (mm/s)	22.2 ± 19.4	118.4 ± 52.8	< **0.001*** [c]
	IMBAV ML (mm/s)	54.7 ± 40.1	137.4 ± 69.9	< **0.001*** [c]
	IMBMV (mm/s)	125.9 ± 77.4	379.1 ± 171.2	< **0.001*** [c]
	IMBMV AP (mm/s)	59.0 ± 37.8	264.4 ± 120.4	< **0.001*** [c]
	IMBMV ML (mm/s)	114.5 ± 73.6	287.6 ± 134.1	< **0.001*** [b]
	UNLT (s)	0.76 ± 0.33	0.35 ± 0.08	< **0.001*** [c]
	UNLD AP (mm)	−1.3 ± 26.9	−12.3 ± 17.9	0.126[b]
	UNLAV AP (mm/s)	37.9 ± 35.4	57.3 ± 29.7	0.044[c]
	UNLMV AP (mm/s)	187.7 ± 87.6	366.4 ± 172.1	0.005[c]
	UNLCoMV (mm/s)	108.5 ± 36.5	222.1 ± 74.4	< **0.001***[c]
	UNLCoMA (mm/s^2)	765.8 ± 295.1	1450.0 ± 452.2	< **0.001***[b]
	UNLCoPCoM (mm)	50.8 ± 20.2	85.0 ± 32.8	0.007[b]
	UNLSLOPE (°)	64.4 ± 15.9	39.9 ± 12.3	< **0.001***[b]
	TOCoMV (mm/s)	325.3 ± 134.9	864.3 ± 185.5	< **0.001***[c]
	TOCoMA (mm/s^2)	849.7 ± 330.8	1178.8 ± 375.4	0.057[c]
	TOCoPCoM (mm)	158.2 ± 76.0	304.3 ± 62.0	< **0.001***[c]
	SL (mm)	297.9 ± 95.4	553.6 ± 90.2	< **0.001***[b]
	SAV (mm/s)	349.3 ± 143.9	1010.8 ± 138.3	< **0.001***[b]
	SMV (mm/s)	1972.1 ± 819.9	3112.9 ± 522.2	< **0.001***[b]

See Table 1 for definitions of GI parameters. Data are shown as mean ± standard deviation. [a] Pearson's chi-squared test, [b] Student's t-test, [c] Wilcoxon rank-sum test. * significant p values after Bonferroni correction. The IMBD ML was defined positive when the CoP was moving towards the swing foot, while the UNLD ML was defined positive when the CoP displacement was towards the stance foot. We considered both the IMBD AP and UNLD AP positive when the CoP displacement was oriented backwards. Abbreviations: GI = gait initiation, HC = healthy controls, LEDD = levodopa equivalent daily dose, PSP = progressive supranuclear palsy cohort, PSPRS = Progressive Supranuclear Palsy Rating Scale.

(Table 2). These biomechanical findings were corroborated by the correlation with the PSPRS subscores Limb motor and Gait and Midline (Table 3A), thus supporting the utility of this clinical scale to detect GI abnormalities and potentially predict the risk of fall in PSP (Bluett et al., 2017).

Overall, the observed biomechanical pattern of GI in patients with PSP suggests impaired modulation of the CoP-CoM coupling for a proper setting of CoM momentum. This activity is directly top-down controlled by the supraspinal locomotor network (Herr and Popovic, 2008; Honeine et al., 2014; Popovic et al., 2004), which is capable of regulating the gravitational disequilibrium torque acting on the CoM for efficient stepping, according to ego- and allocentric spatial reference frames. In particular, our findings suggest a predominant role of the caudate nucleus in the planning and execution of the GI program. This is in agreement with our previous study, where we showed a specific contribution of striatal dopamine to the IMB and step execution at the GI of patients with Parkinson's disease (PD) (Palmisano et al., 2020). Also, patients with PD and postural instability (Rosenberg-Katz et al., 2013) showed caudate atrophy and decreased functional connectivity between the caudate nucleus and SMA, an area directly involved in APA production (Jacobs et al., 2009; MacKinnon et al., 2007). Of note, the basal ganglia have strong anatomical and functional connections with the cortex, thalamus, and brainstem, and play a relevant role in initiating and controlling locomotion (Arnulfo et al., 2018; Isaias et al., 2012; Palmisano et al., 2020; Pozzi et al., 2019; Takakusaki, 2017).

In our study, we also showed a contribution of the cingulate cortex to GI. Hypometabolism of this brain area correlated significantly with the CoM velocity at the end of the UNL (Table 3A, Fig. 3) and with near significance for several other measurements (i.e., IMBAV, UNLT, TOCoPCoM). The cingulate cortex has widespread anatomical projections to the prefrontal cortex, premotor area, parietal lobe, striatum, amygdala, and hypothalamus (Beckmann et al., 2009). It relates to a variety of movement-relevant functions, including executive and attentive function, decision making, and performance monitoring (Bubb et al.,

Table 3
Significant correlations of gait initiation parameters with PSPRS subscores (A) and [18F]FDG-PET findings (B) in patients with PSP.

A	History		Mentation		Bulbar		Ocular motor		Limb motor		Gait and midline		Total	
GI parameters	rho	p-val	rho	p-val	rho	p-val	rho	p-val	rho	p-val	rho	p-val	rho	p-val
IMBT	*0.226*	*0.457*	*−0.186*	*0.543*	*0.005*	*0.988*	*0.189*	*0.537*	*0.311*	*0.301*	*0.036*	*0.906*	*0.257*	*0.397*
IMBD	−0.106	0.719	−0.326	0.255	−0.137	0.640	−0.018	0.952	−0.339	0.236	−0.164	0.575	−0.209	0.473
IMBD AP	−0.371	0.191	−0.002	0.994	−0.324	0.259	−0.446	0.110	−0.465	0.094	−0.442	0.114	−0.482	0.081
IMBD ML	−0.263	0.363	−0.230	0.428	−0.135	0.646	0.033	0.910	−0.404	0.152	−0.273	0.345	−0.269	0.353
IMBAV	−0.448	0.108	−0.249	0.392	−0.135	0.646	−0.127	0.665	−0.512	0.061	−0.335	0.241	−0.436	0.119
IMBAV AP	−0.194	0.507	−0.153	0.602	−0.488	0.077	−0.276	0.339	−0.433	0.122	−0.522	0.056	−0.493	0.073
IMBAV ML	−0.459	0.099	−0.262	0.365	−0.223	0.443	−0.111	0.705	−0.577	**0.031***	−0.426	0.129	−0.491	0.074
IMBMV	−0.344	0.228	−0.294	0.308	−0.184	0.529	−0.065	0.826	−0.379	0.181	−0.291	0.313	−0.333	0.245
IMBMV AP	−0.128	0.662	−0.276	0.340	−0.306	0.287	−0.305	0.289	−0.350	0.220	−0.302	0.294	−0.370	0.193
IMBMV ML	−0.295	0.306	−0.235	0.419	−0.088	0.764	−0.098	0.739	−0.424	0.130	−0.184	0.528	−0.324	0.259
UNLT	0.534	**0.049***	0.030	0.920	0.308	0.284	0.113	0.702	0.601	**0.023***	0.591	**0.026***	0.486	0.078
UNLD AP	*−0.295*	*0.306*	*−0.226*	*0.438*	*0.272*	*0.347*	*0.158*	*0.589*	*−0.213*	*0.464*	*0.036*	*0.904*	*−0.053*	*0.858*
UNLAV AP	*−0.479*	*0.083*	*−0.176*	*0.548*	*−0.007*	*0.980*	*−0.299*	*0.300*	*−0.371*	*0.192*	*−0.266*	*0.357*	*−0.403*	*0.153*
UNLMV AP	*−0.441*	*0.132*	*−0.383*	*0.197*	*−0.261*	*0.389*	*−0.402*	*0.174*	*−0.369*	*0.214*	*−0.431*	*0.141*	*−0.540*	*0.057*
UNLCoMV	−0.001	0.996	0.054	0.861	−0.343	0.251	0.080	0.796	0.014	0.963	−0.342	0.253	−0.076	0.806
UNLCoMA	−0.291	0.359	0.011	0.973	0.063	0.846	−0.243	0.448	−0.413	0.182	−0.155	0.630	−0.399	0.198
UNLCoPCoM	*−0.227*	*0.455*	*−0.020*	*0.947*	*−0.386*	*0.193*	*−0.313*	*0.298*	*−0.588*	*0.035**	*−0.532*	*0.061*	*−0.454*	*0.119*
UNLSLOPE	0.272	0.368	−0.289	0.338	−0.054	0.862	−0.383	0.197	−0.124	0.687	0.206	0.500	−0.195	0.523
TOCOMV	−0.247	0.438	−0.305	0.334	−0.497	0.100	−0.082	0.801	−0.368	0.239	−0.586	**0.045***	−0.415	0.180
TOCOMA	*−0.161*	*0.618*	*−0.150*	*0.641*	*−0.338*	*0.282*	*−0.007*	*0.983*	*−0.011*	*0.973*	*−0.300*	*0.344*	*−0.224*	*0.484*
TOCoPCoM	0.182	0.571	0.070	0.830	−0.370	0.237	0.452	0.140	0.360	0.251	−0.265	0.406	0.112	0.729
SL	−0.285	0.323	−0.160	0.585	−0.252	0.386	0.227	0.434	0.070	0.813	−0.407	0.149	0.000	1.000
SAV	−0.481	0.082	−0.048	0.871	−0.191	0.512	0.153	0.602	−0.173	0.554	−0.496	0.072	−0.117	0.691
SMV	−0.209	0.473	0.103	0.727	−0.517	0.058	0.270	0.351	−0.007	0.982	−0.573	**0.032***	−0.035	0.905

B	Left caudate		Medial thalamus		DLPFC		Left SMA		Mid cingulum		Midbrain	
GI parameters	rho	p-val	rho	p-val	rho	p-val	rho	p-val	rho	p-val	rho	p-val
IMBT	*−0.455*	*0.159*	*−0.3*	*0.37*	*−0.391*	*0.235*	*−0.213*	*0.53*	*−0.853*	*0.001**	*−0.101*	*0.768*
IMBD	0.269	0.424	0.009	0.979	−0.228	0.501	0.257	0.446	0.393	0.232	−0.127	0.709
IMBD AP	0.424	0.194	0.046	0.894	0.264	0.432	0.486	0.129	0.224	0.508	0.027	0.937
IMBD ML	0.255	0.449	0.032	0.925	−0.21	0.536	0.284	0.397	0.466	0.149	−0.027	0.937
IMBAV	0.401	0.222	0.147	0.667	−0.132	0.699	0.303	0.365	0.594	0.054	0.036	0.915
IMBAV AP	0.665	**0.026***	0.201	0.553	0.041	0.905	0.551	0.079	0.566	0.069	0.027	0.937
IMBAV ML	0.324	0.332	0.096	0.779	−0.169	0.62	0.248	0.463	0.562	0.072	0.055	0.873
IMBMV	0.415	0.205	0.142	0.677	−0.214	0.527	0.229	0.497	0.553	0.078	0.091	0.79
IMBMV AP	0.442	0.174	−0.028	0.936	0.128	0.709	0.569	0.068	0.347	0.296	−0.273	0.417
IMBMV ML	0.255	0.449	0.082	0.81	−0.205	0.545	0.266	0.429	0.498	0.119	0.046	0.894
UNLT	−0.532	0.092	−0.358	0.28	0.091	0.789	−0.028	0.936	−0.595	0.054	−0.351	0.29
UNLD AP	*−0.424*	*0.194*	*−0.11*	*0.748*	*−0.579*	*0.062*	*−0.422*	*0.196*	*−0.429*	*0.188*	*−0.027*	*0.937*
UNLAV AP	*0.396*	*0.228*	*0.096*	*0.779*	*0.232*	*0.492*	*0.312*	*0.35*	*0.192*	*0.572*	*−0.164*	*0.631*
UNLMV AP	*−0.037*	*0.92*	*−0.39*	*0.265*	*−0.164*	*0.65*	*0.485*	*0.156*	*−0.366*	*0.298*	*−0.297*	*0.405*
UNLCoMV	0.809	**0.005***	0.502	0.14	0.13	0.721	0.087	0.811	0.644	**0.044***	0.369	0.294
UNLCoMA	0.316	0.374	0.098	0.789	0.037	0.92	0.534	0.112	0.262	0.464	0.018	0.96
UNLCoPCoM	*0.344*	*0.331*	*−0.099*	*0.785*	*−0.102*	*0.779*	*0.413*	*0.236*	*0.183*	*0.612*	*−0.086*	*0.812*
UNLSLOPE	0.231	0.521	−0.22	0.542	0.292	0.413	0.718	**0.019***	0.25	0.486	−0.43	0.214
TOCOMV	0.628	0.07	0.234	0.544	−0.008	0.983	0.288	0.452	0.487	0.183	0.183	0.637
TOCOMA	*0.879*	*0.002**	*0.494*	*0.177*	*0.251*	*0.515*	*0.356*	*0.347*	*0.756*	*0.018**	*0.467*	*0.205*
TOCoPCoM	0.745	**0.021***	0.753	**0.019***	−0.034	0.932	0.102	0.795	0.656	0.055	0.7	**0.036***
SL	0.524	0.098	0.188	0.581	−0.333	0.318	−0.174	0.608	0.219	0.517	0.3	0.37
SAV	0.46	0.154	0.256	0.447	−0.169	0.62	−0.073	0.83	0.365	0.269	0.246	0.467
SMV	0.433	0.184	0.266	0.43	−0.196	0.564	−0.101	0.768	0.151	0.658	0.446	0.17

See Table 1 for definitions of GI parameters. Abbreviations: [18F]FDG = 2-deoxy-2-[18F]fluoro-D-glucose, GI = gait initiation, LEDD = levodopa equivalent daily dose, PET = positron emission tomography, PSPRS = Progressive Supranuclear Palsy Rating Scale, VOI = volume of interest. * significant p values uncorrected ($p < 0.05$). No significant correlation after Bonferroni correction. The values in italic show the biomechanical parameters that did not differ significantly between PSP and HC after Bonferroni correction (see Table 2).

2018). With regards to locomotion, the contribution of the anterior cingulate cortex is still unclear but it could favor the encoding of feedback signals (e.g., trajectory error detection) and contextual information for online adjustment and fine tuning of the gait pattern (Gwin et al., 2011; Hinton et al., 2019; la Fougère et al., 2010; Rosso et al., 2015; Tard et al., 2015). In conjunction with the SMA, the cingulate cortex can favor a shift from steady-state locomotion to more controlled gait (Hinton et al., 2019), and therefore also influence the programming of the GI task regulating APA production. The SMA has specifically been further shown to correlate with the greatest between-step changes to gait phasing (Hinton et al., 2019) and precision stepping (Koenraadt et al., 2014). Mihara and coll. (Mihara et al., 2008) identified the SMA as involved in balance control. Indeed in our study, [18F]FDG uptake of the SMA correlated with the slope of the CoP-CoM vector at UNL end (UNLSLOPE) in PSP patients (Fig. 3) – a GI strategy favoring stability over mobility at first step (i.e., lateral rather than forward movement of the CoM).

Thalamic and midbrain hypometabolism correlated with the distance between CoP and CoM at stance foot toe-off (TOCoPCoM) (Table 3B, Fig. 3). The thalamus has a central role during locomotion

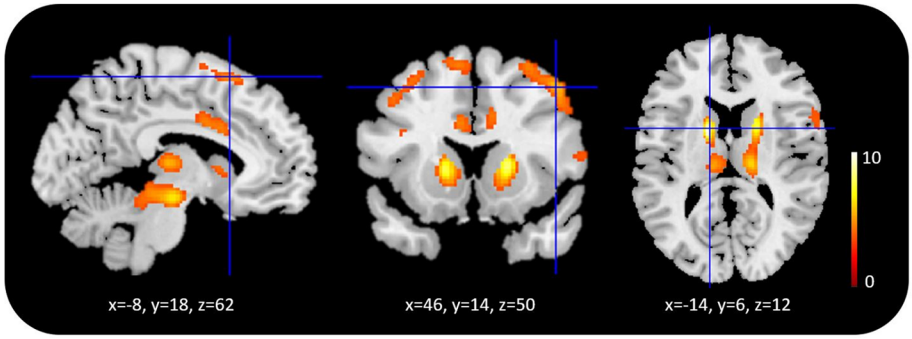

Fig. 2. Brain areas with reduced [18F]FDG uptake in patients with PSP. Patients with PSP showed six hypometabolic brain regions: the left supplementary motor area, the right dorsolateral prefrontal cortex, the left caudate nucleus, the middle cingulate cortex, and the medial thalamus, and the midbrain. The cluster peak coordinates in Montreal Neurological Institute space are listed in the text. In the figure, we show the coordinates of the targeted brain area (blue lines intersection).

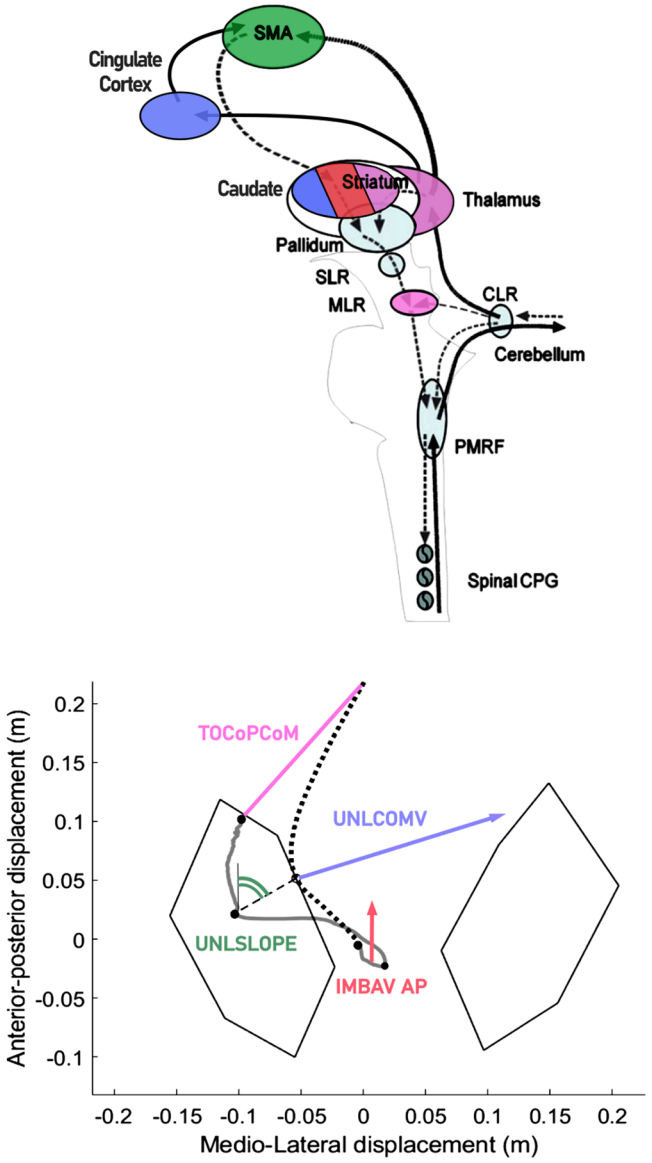

Fig. 3. Overview of the brain network failure at gait initiation in patients with PSP. Schematic representation of the locomotor network (adapted from la Fougère et al., 2010 (la Fougère et al., 2010) and Hinton et al., 2019 (Hinton et al., 2019)) with color-coding of impaired brain areas (top) and the related pathological biomechanical resultants (bottom, see also Fig. 1A) during gait initiation in PSP patients. CPG: Central Pattern Generator; CLR: cerebellar locomotor region; MLR: mesencephalic locomotor region; PMRF: pontine and medullary reticular formations; PSP: progressive supranuclear palsy; SLR: subthalamic locomotor region; SMA: supplementary motor area. See Table 1 for definitions of GI parameters.

and particularly during gait modulation, stepping on a complex terrain and upon transition from standing to walking (Marlinski et al., 2012; Takakusaki, 2017). It conveys and integrates the locomotion-related information of the basal ganglia with the cerebellar and somatosensory inputs, and directly modulates the activity of the motor cortex in different phases of the step cycle (Marlinski et al., 2012). In PSP patients, reduced functional connectivity was observed between the thalamus and several brain areas of the locomotor network, including the SMA, striatum, and cerebellum, independently from grey matter atrophy (Whitwell et al., 2012). Also in these patients, posturography analysis combined with resting state PET with [18F]FDG showed a correlation between high values of the CoP sway path and decreased glucose uptake in the thalamus and in the caudate nucleus. The thalamus was the only region where this correlation markedly increased during modulation of sensory input (i.e., eyes open/close and head straight/extended) (Zwergal et al., 2011). While the basal ganglia are primarily involved in APA programming for subsequent motor actions, the thalamus may therefore subserve optimization of the stepping phase by integrating the basal ganglia output with ascending somatosensory and cerebellar information (Takakusaki, 2017).

The mesencephalic (or midbrain) locomotor region (MLR) is a cornerstone brain area in the supraspinal locomotor network. It receives inputs from the cortex, the basal ganglia, and the cerebellum, and projects to ascending thalamocortical and descending reticulospinal pathways (Pahapill and Lozano, 2000). The precise anatomical delineations of this brain area and the functional interplay of its main regions (the pedunculopontine nucleus [PPN] and cuneiform nucleus [CN]) remain unclear, especially in the context of human gait. With regard to human studies, mesencephalic activations are observed during the imagination of gait (Snijders et al., 2011), especially in a speed-dependent context (Jahn et al., 2008; Karachi et al., 2012). Demain and coll. showed in elderly people with “higher-level gait disorders” a negative correlation between grey matter reduction in the MLR and the posterior CoP displacement during APA, which directly related to the severity of falls (Demain et al., 2014). Of interest, the MLR impairment in these patients was mostly related to disrupted coupling of APA and step execution (Eckert et al., 2014). Direct electrophysiological recordings of the sub-cuneiform nucleus during electrode implantation for deep brain stimulation (DBS) in patients with PD and freezing of gait showed that some neurons modulate their firing rate to the velocity of (mimicked) stepping (Piallat et al., 2009). Also in PD, biomechanical analysis of GI showed a direct effect of DBS of the PPN area in normalizing the backward shift and velocity of the CoP during IMB, and the peak velocity during the stepping phase (Mazzone et al., 2014). In our study, we could not find a direct correlation between the midbrain [18F]FDG uptake and IMB measures; however, the positive correlation with the distance between CoP and CoM at stance foot toe-off (TOCoPCoM) supports a gateway role of the MLR for appropriate stepping. It is worth noting that in our study, biomechanical correlations with the midbrain might have been masked by the severe neuronal loss – and consequently reduced [18F]FDG uptake – of this brain area in the PSP patients (Eckert et al., 2005). Furthermore, the

PET resolution prevents precise identification of the anatomical locations of the CN and PPN that are possibly involved in specific functions of GI and human gait in general.

Our study has some limitations. First, the sample size of the PSP group was small, and the biomechanical assessment of GI relied on only a few trials in each patient. However, PSP is a rare disease and patients already display severe balance loss at the time of diagnosis, making biomechanical assessment very difficult. Nevertheless, the sample size is in line with similar studies (Amano et al., 2015; Zwergal et al., 2011). Second, the control groups for the biomechanical and neuroimaging evaluations were different, thus preventing direct comparison for healthy subjects. This is mainly related to the difficulty in performing research studies with radioactive exposure in healthy individuals, which led us to use previously acquired [18F]FDG PET normative data. Finally, biomechanical correlations with neuroimaging results were not significant after the Bonferroni correction for multiple comparisons. This was to be expected, given the large number of variables included. We would therefore recommend caution in the interpretation of our findings, which deserve confirmation in larger cohorts.

In conclusion, our results provide evidence to support the hypothesis that dysfunctional postural control at GI in PSP patients involves poor APA programming and execution. Multiple brain regions of the supraspinal locomotor network specifically contribute in a principled, controlled manner to an efficient GI.

Funding

This study was sponsored in part by the “Fondazione Grigioni per il Morbo di Parkinson” and the Deutsche Forschungsgemeinschaft (DFG, German Research Foundation) – Project-ID 424778381-TRR 295.

CRediT authorship contribution statement

Chiara Palmisano: Methodology, Software, Formal analysis, Investigation, Data curation, Writing - original draft. **Massimiliano Todisco:** Formal analysis, Writing - original draft. **Giorgio Marotta:** Formal analysis, Writing - review & editing. **Jens Volkmann:** Writing - review & editing. **Claudio Pacchetti:** Writing - review & editing. **Carlo A. Frigo:** Writing - review & editing. **Gianni Pezzoli:** Conceptualization, Writing - review & editing, Funding acquisition. **Ioannis U. Isaias:** Conceptualization, Methodology, Formal analysis, Investigation, Resources, Writing - original draft, Supervision, Project administration.

Declaration of Competing Interest

The authors declare that they have no known competing financial interests or personal relationships that could have appeared to influence the work reported in this paper.

Acknowledgements

We would like to thank all patients and caregivers for their participation. We thank Margherita Canesi for referral of patients and Mariangela Dipaola, Virginia Maltese and Alberto Marzegan for data acquisitions and data pre-processing. The draft manuscript was edited for English language by Deborah Nock (Medical WriteAway, Norwich, UK).

References

Amano, S., Skinner, J.W., Lee, H.K., Stegemöller, E.L., Hack, N., Akbar, U., Vaillancourt, D., McFarland, N.R., Hass, C.J., 2015. Discriminating features of gait performance in progressive supranuclear palsy. Park. Relat. Disord. 21, 888–893. https://doi.org/10.1016/j.parkreldis.2015.05.017.

Arnulfo, G., Pozzi, N.G., Palmisano, C., Leporini, A., Canessa, A., Brumberg, J., Pezzoli, G., Matthies, C., Volkmann, J., Isaias, I.U., 2018. Phase matters: A role for the subthalamic network during gait. PLoS One 13, 1–19. https://doi.org/10.1371/journal.pone.0198691.

Beckmann, M., Johansen-Berg, H., Rushworth, M.F.S., 2009. Connectivity-based parcellation of human cingulate cortex and its relation to functional specialization. J. Neurosci. 29, 1175–1190. https://doi.org/10.1523/JNEUROSCI.3328-08.2009.

Bluett, B., Litvan, I., Cheng, S., Juncos, J., Riley, D.E., Standaert, D.G., Reich, S.G., Hall, D. A., Kluger, B., Shprecher, D., Marras, C., Jankovic, J., 2017. Understanding falls in progressive supranuclear palsy. Parkinsonism Relat. Disord. 35, 75–81. doi: 10.1016/j.parkreldis.2016.12.009.

Bubb, E.J., Metzler-Baddeley, C., Aggleton, J.P., 2018. The cingulum bundle: Anatomy, function, and dysfunction. Neurosci. Biobehav. Rev. 92, 104–127. https://doi.org/10.1016/j.neubiorev.2018.05.008.

Canesi, M., Giordano, R., Lazzari, L., Isalberti, M., Isaias, I.U., Benti, R., Rampini, P., Marotta, G., Colombo, A., Cereda, E., Dipaola, M., Montemurro, T., Viganò, M., Budelli, S., Montelatici, E., Lavazza, C., Cortelezzi, A., Pezzoli, G., 2016. Finding a new therapeutic approach for no-option Parkinsonisms: Mesenchymal stromal cells for progressive supranuclear palsy. J. Transl. Med. 14, 1–11. https://doi.org/10.1186/s12967-016-0880-2.

Clerici, I., Ferrazzoli, D., Maestri, R., Bossio, F., Zivi, I., Canesi, M., Pezzoli, G., Frazzitta, G., 2017. Rehabilitation in progressive supranuclear palsy: Effectiveness of two multidisciplinary treatments. PLoS One 12, 1–12. https://doi.org/10.1371/journal.pone.0170927.

Crenna, P., Carpinella, I., Rabuffetti, M., Rizzone, M., Lopiano, L., Lanotte, M., Ferrarin, M., 2006. Impact of subthalamic nucleus stimulation on the initiation of gait in Parkinson’s disease. Exp. Brain Res. 172, 519–532. https://doi.org/10.1007/s00221-006-0360-7.

Demain, A., Westby, G.W.M., Fernandez-Vidal, S., Karachi, C., Bonneville, F., Do, M.C., Delmaire, C., Dormont, D., Bardinet, E., Agid, Y., Chastan, N., Welter, M.L., 2014. High-level gait and balance disorders in the elderly: A midbrain disease? J. Neurol. 261, 196–206. https://doi.org/10.1007/s00415-013-7174-x.

Dipaola, M., Pavan, E.E., Cattaneo, A., Frazzitta, G., Pezzoli, G., Cavallari, P., Frigo, C.A., Isaias, I.U., 2016. Mechanical energy recovery during walking in patients with Parkinson disease. PLoS One 11. https://doi.org/10.1371/journal.pone.0156420.

Eckert, T., Barnes, A., Dhawan, V., Frucht, S., Gordon, M.F., Feigin, A.S., Eidelberg, D., 2005. FDG PET in the differential diagnosis of parkinsonian disorders. Neuroimage 26, 912–921. https://doi.org/10.1016/j.neuroimage.2005.03.012.

Eckert, T., Barnes, A., Dhawan, V., Frucht, S., Gordon, M.F., Feigin, A.S., Eidelberg, D., Jahn, K., Deutschländer, A., Stephan, T., Kalla, R., Wiesmann, M., Strupp, M., Brandt, T., Snijders, A.H., Leunissen, I., Bakker, M., Overeem, S., Helmich, C., Bloem, B.R., Toni, I., Tard, C., Delval, A., Devos, D., Lopes, R., Lenfant, P., Dujardin, K., Hossein-Foucher, C., Semah, F., Duhamel, A., Defebvre, L., Le Jeune, F., Moreau, C., Pahapill, P.A., Lozano, A.M., Bubb, E.J., Metzler-Baddeley, C., Aggleton, J.P., Demain, A., Westby, G.W.M., Fernandez-Vidal, S., Karachi, C., Bonneville, F., Do, M.C., Delmaire, C., Dormont, D., Bardinet, E., Agid, Y., Chastan, N., Welter, M.L., Manuscript, A., Karachi, C., André, A., Bertasi, E., Bardinet, E., Lehéricy, S., Bernard, F.A., la Fougère, C., Zwergal, A., Rominger, A., Förster, S., Fesl, G., Dieterich, M., Brandt, T., Strupp, M., Bartenstein, P., Jahn, K., Mazzone, P., Paoloni, M., Mangone, M., Santilli, V., Insola, A., Fini, M., Scarnati, E., Piallat, B., Chabardès, S., Torres, N., Fraix, V., Goetz, L., Seigneuret, E., Bardinet, E., Ferraye, M., Debu, B., Krack, P., Yelnik, J., Pollak, P., Benabid, A.L., Hinton, D.C., Thiel, A., Soucy, J.P., Bouyer, L., Paquette, C., 2014. Functional parcellation of the lateral mesencephalus. Neuroimage 50, 104–127. https://doi.org/10.1016/j.neubiorev.2018.05.008.

Farinelli, V., Palmisano, C., Marchese, S.M., Strano, C.M.M., D'Arrigo, S., Pantaleoni, C., Ardissone, A., Nardocci, N., Esposti, R., Cavallari, P., 2020. Postural Control in Children with Cerebellar Ataxia. Appl. Sci. 10, 1606. https://doi.org/10.3390/app10051606.

Fawver, B., Roper, J.A., Sarmento, C., Hass, C.J., 2018. Forward leaning alters gait initiation only at extreme anterior postural positions. Hum. Mov. Sci. 59, 1–11. https://doi.org/10.1016/j.humov.2018.03.006.

Foster, N.L., Gilman, S., Berent, S., Morin, E.M., Brown, M.B., Koeppe, R.A., 1988. Cerebral hypometabolism in progressive supranuclear palsy studied with positron emission tomography. Ann. Neurol. 24, 399–406. https://doi.org/10.1002/ana.410240308.

Giordano, R., Canesi, M., Isalberti, M., Isaias, I.U., Montemurro, T., Viganò, M., Montelatici, E., Boldrin, V., Benti, R., Cortelezzi, A., Fracchiolla, N., Lazzari, L., Pezzoli, G., 2014. Autologous mesenchymal stem cell therapy for progressive supranuclear palsy: Translation into a phase I controlled, randomized clinical study. J. Transl. Med. 12. https://doi.org/10.1186/1479-5876-12-14.

Golbe, L.I., Ohman-Strickland, P.A., 2007. A clinical rating scale for progressive supranuclear palsy. Brain 130, 1552–1565. https://doi.org/10.1093/brain/awm032.

Gwin, J.T., Gramann, K., Makeig, S., Ferris, D.P., 2011. Electrocortical activity is coupled to gait cycle phase during treadmill walking. Neuroimage 54, 1289–1296. https://doi.org/10.1016/j.neuroimage.2010.08.066.

Herr, H., Popovic, M., 2008. Angular momentum in human walking. J. Exp. Biol. 211, 467–481. https://doi.org/10.1242/jeb.008573.

Hinton, D.C., Thiel, A., Soucy, J.P., Bouyer, L., Paquette, C., 2019. Adjusting gait step-by-step: Brain activation during split-belt treadmill walking. Neuroimage 202. https://doi.org/10.1016/j.neuroimage.2019.116095.

Höglinger, G.U., Respondek, G., Stamelou, M., Kurz, C., Josephs, K.A., Lang, A.E., Mollenhauer, B., Müller, U., Nilsson, C., Whitwell, J.L., Arzberger, T., Englund, E., Gelpi, E., Giese, A., Irwin, D.J., Meissner, W.G., Pantelyat, A., Rajput, A., van Swieten, J.C., Troakes, C., Antonini, A., Bhatia, K.P., Bordelon, Y., Compta, Y., Corvol, J.-C., Colosimo, C., Dickson, D.W., Dodel, R., Ferguson, L., Grossman, M., Kassubek, J., Krismer, F., Levin, J., Lorenzl, S., Morris, H.R., Nestor, P., Oertel, W.H., Poewe, W., Rabinovici, G., Rowe, J.B., Schellenberg, G.D., Seppi, K., van Eimeren, T.,

Wenning, G.K., Boxer, A.L., Golbe, L.I., Litvan, I., Group, M.D.S.P.S.P.S., 2017. Clinical diagnosis of progressive supranuclear palsy: The movement disorder society criteria. Mov. Disord. 32, 853–864. doi: 10.1002/mds.26987.

Honeine, J.-L., Schieppati, M., Gagey, O., Do, M.-C., 2014. By counteracting gravity, triceps surae sets both kinematics and kinetics of gait. Physiol. Rep. 2, e00229. https://doi.org/10.1002/phy2.229.

Isaias, I.U., Brumberg, J., Pozzi, N.G., Palmisano, C., Canessa, A., Marotta, G., Volkmann, J., Pezzoli, G., 2020. Brain metabolic alterations herald falls in patients with Parkinson' s disease. Ann. Clin. Transl. Neurol. 1–5. https://doi.org/10.1002/acn3.51013.

Isaias, I.U., Dipaola, M., Michi, M., Marzegan, A., Volkmann, J., Roidi, M.L.R., Frigo, C.A., Cavallari, P., 2014. Gait initiation in children with Rett syndrome. PLoS One 9. https://doi.org/10.1371/journal.pone.0092736.

Isaias, I.U., Volkmann, J., Marzegan, A., Marotta, G., Cavallari, P., Pezzoli, G., 2012. The Influence of Dopaminergic Striatal Innervation on Upper Limb Locomotor Synergies. PLoS One 7, 3–6. https://doi.org/10.1371/journal.pone.0051464.

Jacobs, J.V., Lou, J.S., Kraakevik, J.A., Horak, F.B., 2009. The supplementary motor area contributes to the timing of the anticipatory postural adjustment during step initiation in participants with and without Parkinson's disease. Neuroscience 164, 877–885. https://doi.org/10.1016/j.neuroscience.2009.08.002.

Jahn, K., Deutschländer, A., Stephan, T., Kalla, R., Wiesmann, M., Strupp, M., Brandt, T., 2008. Imaging human supraspinal locomotor centers in brainstem and cerebellum. Neuroimage 39, 786–792. https://doi.org/10.1016/j.neuroimage.2007.09.047.

Karachi, C., André, A., Bertasi, E., Bardinet, E., Lehéricy, S., Bernard, F.A., 2012. Functional parcellation of the lateral mesencephalus. J. Neurosci. 32, 9396–9401. https://doi.org/10.1523/JNEUROSCI.0509-12.2012.

Karbe, H., Grond, M., Huber, M., Herholz, K., Kessler, J., Heiss, W.D., 1992. Subcortical damage and cortical dysfunction in progressive supranuclear palsy demonstrated by positron emission tomography. J. Neurol. 239, 98–102. https://doi.org/10.1007/BF00862982.

Koenraadt, K.L.M., Roelofsen, E.G.J., Duysens, J., Keijsers, N.L.W., 2014. Cortical control of normal gait and precision stepping: An fNIRS study. Neuroimage 85, 415–422. https://doi.org/10.1016/j.neuroimage.2013.04.070.

la Fougère, C., Zwergal, A., Rominger, A., Förster, S., Fesl, G., Dieterich, M., Brandt, T., Strupp, M., Bartenstein, P., Jahn, K., 2010. Real versus imagined locomotion: A [18F]-FDG PET-fMRI comparison. Neuroimage 50, 1589–1598. https://doi.org/10.1016/j.neuroimage.2009.12.060.

MacKinnon, C.D., Bissig, D., Chiusano, J., Miller, E., Rudnick, L., Jager, C., Zhang, Y., Mille, M.L., Rogers, M.W., 2007. Preparation of anticipatory postural adjustments prior to stepping. J. Neurophysiol. 97, 4368–4379. https://doi.org/10.1152/jn.01136.2006.

Marlinski, V., Nilaweera, W.U., Zelenin, P.V., Sirota, M.G., Beloozerova, I.N., 2012. Signals from the ventrolateral thalamus to the motor cortex during locomotion. J. Neurophysiol. 107, 455–472. https://doi.org/10.1152/jn.01113.2010.

Mazzone, P., Paoloni, M., Mangone, M., Santilli, V., Insola, a, Fini, M., Scarnati, E., 2014. Unilateral deep brain stimulation of the pedunculopontine tegmental nucleus in idiopathic Parkinson's disease: Effects on gait initiation and performance. Gait Posture 40, 357–62. doi: 10.1016/j.gaitpost.2014.05.002.

McIlroy, W.E., Maki, B.E., 1999. The control of lateral stability during rapid stepping reactions evoked by antero-posterior perturbation: Does anticipatory control play a role? Gait Posture 9, 190–198. https://doi.org/10.1016/S0966-6362(99)00013-2.

Mihara, M., Miyai, I., Hatakenaka, M., Kubota, K., Sakoda, S., 2008. Role of the prefrontal cortex in human balance control. Neuroimage 43, 329–336. https://doi.org/10.1016/j.neuroimage.2008.07.029.

O'Malley, M.J., 1996. Normalization of temporal-distance parameters in pediatric gait. J. Biomech. 29, 619–625.

Pahapill, P.A., Lozano, A.M., 2000. The pedunculopontine nucleus and Parkinson ' s disease. Brain 123, 1767–1783.

Palmisano, C., Brandt, G., Pozzi, N.G., Alice, L., Maltese, V., Andrea, C., Jens, V., Pezzoli, G., Frigo, C.A., Isaias, I.U., 2019. Sit-to-walk performance in Parkinson's disease: a comparison between faller and non-faller patients. Clin. Biomech. doi: 10.1016/j.clinbiomech.2019.03.002.

Palmisano, C., Brandt, G., Vissani, M., Pozzi, N.G., Canessa, A., Brumberg, J., Marotta, G., Volkmann, J., Mazzoni, A., Pezzoli, G., Frigo, C.A., Isaias, I.U., 2020. Gait initiation in Parkinson's disease: impact of dopamine depletion and initial stance condition. Front. Bioeng. Biotechnol. 8, 1–9. https://doi.org/10.3389/fbioe.2020.00137.

Piallat, B., Chabardès, S., Torres, N., Fraix, V., Goetz, L., Seigneuret, E., Bardinet, E., Ferraye, M., Debu, B., Krack, P., Yelnik, J., Pollak, P., Benabid, A.L., 2009. Gait is associated with an increase in tonic firing of the sub-cuneiform nucleus neurons. Neuroscience 158, 1201–1205. https://doi.org/10.1016/j.neuroscience.2008.10.046.

Popovic, M., Hofmann, A., Herr, H., 2004. Angular momentum regulation during human walking: Biomechanics and control. Proc. - IEEE Int. Conf. Robot. Autom. 2004, 2405–2411. https://doi.org/10.1109/robot.2004.1307421.

Pozzi, N.G., Canessa, A., Palmisano, C., Brumberg, J., Steigerwald, F., Reich, M.M., Minafra, B., Pacchetti, C., Pezzoli, G., Volkmann, J., Isaias, I.U., 2019. Freezing of gait in Parkinson's disease reflects a sudden derangement of locomotor network dynamics. Brain 142, 2037–2050. https://doi.org/10.1093/brain/awz141.

Respondek, G., Stamelou, M., Kurz, C., Ferguson, L.W., Rajput, A., Chiu, W.Z., van Swieten, J.C., Troakes, C., al Sarraj, S., Gelpi, E., Gaig, C., Tolosa, E., Oertel, W.H., Giese, A., Roeber, S., Arzberger, T., Wagenpfeil, S., Höglinger, G.U., 2014. The phenotypic spectrum of progressive supranuclear palsy: A retrospective multicenter study of 100 definite cases. Mov. Disord. 29, 1758–1766. doi: 10.1002/mds.26054..

Richard, A., Van Hamme, A., Drevelle, X., Golmard, J.L., Meunier, S., Welter, M.L., 2017. Contribution of the supplementary motor area and the cerebellum to the anticipatory postural adjustments and execution phases of human gait initiation. Neuroscience 358, 181–189. https://doi.org/10.1016/j.neuroscience.2017.06.047.

Rocchi, L., Chiari, L., Mancini, M., Carlson-Kuhta, P., Gross, A., Horak, F.B., 2006. Step initiation in Parkinson's disease: Influence of initial stance conditions. Neurosci. Lett. 406, 128–132. https://doi.org/10.1016/j.neulet.2006.07.027.

Rosenberg-Katz, K., Herman, T., Jacob, Y., Giladi, N., Hendler, T., Hausdorff, J.M., 2013. Gray matter atrophy distinguishes between Parkinson disease motor subtypes. Neurology 80, 1476–1484. https://doi.org/10.1212/WNL.0b013e31828cfaa4.

Rosso, A.L., Hunt, M.J.O., Yang, M., Brach, J.S., Harris, T.B., Newman, A.B., Satterfield, S., Studenski, S.A., Yaffe, K., Howard, J., 2015. Higher Step Length Variability Indicates Lower Grey Matter Integrity of Selected Regions in Older Adults 40, 225–230. doi: 10.1016/j.gaitpost.2014.03.192.Higher.

Snijders, A.H., Leunissen, I., Bakker, M., Overeem, S., Helmich, C., Bloem, B.R., Toni, I., 2011. Gait-related cerebral alterations in patients with Parkinson ' s disease with freezing of gait. doi: 10.1093/brain/awq324.

Takakusaki, K., 2017. Functional neuroanatomy for posture and gait control. J. Mov. Disord. 10, 1–17. https://doi.org/10.14802/jmd.16062.

Tard, C., Delval, A., Devos, D., Lopes, R., Lenfant, P., Dujardin, K., Hossein-Foucher, C., Semah, F., Duhamel, A., Defebvre, L., Le Jeune, F., Moreau, C., 2015. Brain metabolic abnormalities during gait with freezing in Parkinson's disease. Neuroscience 307, 281–301. https://doi.org/10.1016/j.neuroscience.2015.08.063.

Welter, M.L., Do, M.C., Chastan, N., Torny, F., Bloch, F., Tézenas du Montcel, S., Agid, Y., 2007. Control of vertical components of gait during initiation of walking in normal adults and patients with progressive supranuclear palsy. Gait Posture 26, 393–399. https://doi.org/10.1016/j.gaitpost.2006.10.005.

Whitwell, J.L., Xu, J., Mandrekar, J., Gunter, J.L., Jack, C.R., Josephs, K.A., 2012. Imaging measures predict progression in progressive supranuclear palsy. Mov. Disord. 27, 1801–1804. https://doi.org/10.1002/mds.24970.

Winter, D.A., 1995. Human balance and posture control during standing and walking. Gait Posture 3, 193–214. https://doi.org/10.1016/0966-6362(96)82849-9.

Yiou, E., Caderby, T., Delafontaine, A., Fourcade, P., Honeine, J.-L.L., 2017. Balance control during gait initiation: State-of-the-art and research perspectives. World J. Orthop. 8, 815–828. https://doi.org/10.5312/wjo.v8.i11.815.

Zatsiorsky, V.M., 2002. Kinetics of Human Motion. Human Kinetics.

Zwergal, A., La Fougère, C., Lorenzl, S., Rominger, a., Xiong, G., Deutschenbaur, L., Linn, J., Krafczyk, S., Dieterich, M., Brandt, T., Strupp, M., Bartenstein, P., Jahn, K., 2011. Postural imbalance and falls in PSP correlate with functional pathology of the thalamus. Neurology 77, 101–109. doi: 10.1212/WNL.0b013e318223c79d.